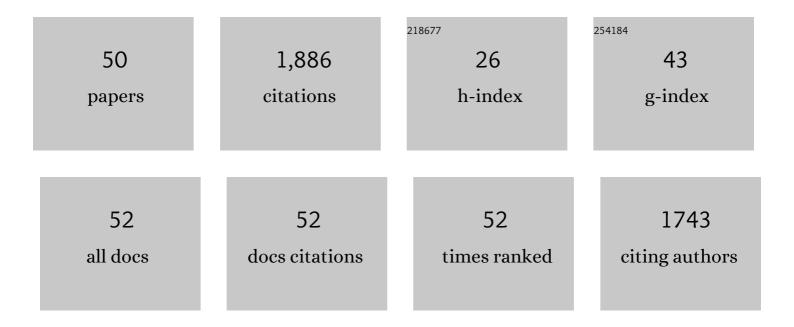
## Federico Tasca

List of Publications by Year in descending order

Source: https://exaly.com/author-pdf/4364376/publications.pdf Version: 2024-02-01



FEDERICO TASCA

#	Article	IF	CITATIONS
1	Activity volcano plots for the oxygen reduction reaction using FeN4 complexes: From reported experimental data to the electrochemical meaning. Current Opinion in Electrochemistry, 2022, 32, 100923.	4.8	12
2	Evidence of carbon-supported porphyrins pyrolyzed for the oxygen reduction reaction keeping integrity. Scientific Reports, 2022, 12, 8072.	3.3	13
3	Penta-coordinated transition metal macrocycles as electrocatalysts for the oxygen reduction reaction. Journal of Solid State Electrochemistry, 2021, 25, 15-31.	2.5	22
4	Electrochemical reduction of Cr(VI) in the presence of sodium alginate and its application in water purification. Journal of Environmental Sciences, 2021, 101, 304-312.	6.1	32
5	Electrodeposition of Cu2O nanostructures with improved semiconductor properties. Cogent Engineering, 2021, 8, 1875534.	2.2	7
6	Insights into the electronic structure of Fe penta-coordinated complexes. Spectroscopic examination and electrochemical analysis for the oxygen reduction and oxygen evolution reactions. Journal of Materials Chemistry A, 2021, 9, 23802-23816.	10.3	27
7	Oxygen reduction reaction on a 68-atom-gold cluster supported on carbon nanotubes: theoretical and experimental analysis. Materials Chemistry Frontiers, 2021, 5, 7529-7539.	5.9	6
8	Imogolite: a nanotubular aluminosilicate: synthesis, derivatives, analogues, and general and biological applications. Materials Chemistry Frontiers, 2021, 5, 6779-6802.	5.9	12
9	Novel Nanoarchitectures Based on Lignin Nanoparticles for Electrochemical Eco-Friendly Biosensing Development. Nanomaterials, 2021, 11, 718.	4.1	9
10	Gold Nanoparticles/Carbon Nanotubes and Gold Nanoporous as Novel Electrochemical Platforms for L-Ascorbic Acid Detection: Comparative Performance and Application. Chemosensors, 2021, 9, 229.	3.6	7
11	Influence of cyano substituents on the electron density and catalytic activity towards the oxygen reduction reaction for iron phthalocyanine. The case for Fe(II) 2,3,9,10,16,17,23,24-octa(cyano)phthalocyanine. Electrochemistry Communications, 2020, 118, 106784.	4.7	20
12	Use of a Thermophile Desiccation-Tolerant Cyanobacterial Culture and Os Redox Polymer for the Preparation of Photocurrent Producing Anodes. Frontiers in Bioengineering and Biotechnology, 2020, 8, 900.	4.1	7
13	Biocide Activity of Green Quercetin-Mediated Synthesized Silver Nanoparticles. Nanomaterials, 2020, 10, 909.	4.1	24
14	Oxygen Reduction Reaction at Penta-Coordinated Co Phthalocyanines. Frontiers in Chemistry, 2020, 8, 22.	3.6	37
15	Minimally Invasive Clucose Monitoring Using a Highly Porous Gold Microneedles-Based Biosensor: Characterization and Application in Artificial Interstitial Fluid. Catalysts, 2019, 9, 580.	3.5	66
16	Spectroelectrochemical study revealing the redox potential of human monoamine oxidase A. Electrochimica Acta, 2019, 317, 612-617.	5.2	2
17	Microneedle-based electrochemical devices for transdermal biosensing: a review. Current Opinion in Electrochemistry, 2019, 16, 42-49.	4.8	51
18	Comparison of Direct and Mediated Electron Transfer for Bilirubin Oxidase from Myrothecium Verrucaria. Effects of Inhibitors and Temperature on the Oxygen Reduction Reaction. Catalysts, 2019, 9, 1056.	3.5	14

Federico Tasca

#	Article	IF	CITATIONS
19	In search of the most active MN4 catalyst for the oxygen reduction reaction. The case of perfluorinated Fe phthalocyanine. Journal of Materials Chemistry A, 2019, 7, 24776-24783.	10.3	52
20	Amperometric Flow Injection Analysis of Glucose and Galactose Based on Engineered Pyranose 2â€Oxidases and Osmium Polymers for Biosensor Applications. Electroanalysis, 2018, 30, 1496-1504.	2.9	16
21	Adsorption of 4,4′â€Dithiodipyridine Axially Coordinated to Iron(II) Phthalocyanine on Au(111) as a New Strategy for Oxygen Reduction Electrocatalysis. ChemPhysChem, 2018, 19, 1599-1604.	2.1	12
22	Biomimicking vitamin B12. A Co phthalocyanine pyridine axial ligand coordinated catalyst for the oxygen reduction reaction. Electrochimica Acta, 2018, 265, 547-555.	5.2	56
23	(Invited) Climbing over the Activity Volcano Correlation by Biomimicking Vitamin B12: A Co Phthalocyanine Pyridine Axial Ligand Coordinated Catalyst for the Reduction of Molecular Oxygen. ECS Transactions, 2018, 85, 111-121.	0.5	4
24	Biomimetic reduction of O <sub>2</sub> in an acid medium on iron phthalocyanines axially coordinated to pyridine anchored on carbon nanotubes. Journal of Materials Chemistry A, 2017, 5, 12054-12059.	10.3	76
25	Surface Structure of 4-Mercaptopyridine on Au(111): A New Dense Phase. Langmuir, 2017, 33, 9565-9572.	3.5	24
26	Comparison of the catalytic activity for O <sub>2</sub> reduction of Fe and Co MN4 adsorbed on graphite electrodes and on carbon nanotubes. Physical Chemistry Chemical Physics, 2017, 19, 20441-20450.	2.8	45
27	Spectroscopic and Electrochemical Studies of Imogolite and Fe-Modified Imogolite Nanotubes. Nanomaterials, 2016, 6, 28.	4.1	11
28	Reactivity indexes for the electrocatalytic oxidation of hydrogen peroxide promoted by several ligand-substituted and unsubstituted Co phthalocyanines adsorbed on graphite. Journal of Electroanalytical Chemistry, 2016, 765, 22-29.	3.8	18
29	Electrochemical Characterization of Graphene and MWCNT Screen-Printed Electrodes Modified with AuNPs for Laccase Biosensor Development. Nanomaterials, 2015, 5, 1995-2006.	4.1	44
30	Bilirubin Oxidase from Myrothecium verrucaria Physically Absorbed on Graphite Electrodes. Insights into the Alternative Resting Form and the Sources of Activity Loss. PLoS ONE, 2015, 10, e0132181.	2.5	30
31	Linear versus volcano correlations for the electrocatalytic oxidation of hydrazine on graphite electrodes modified with MN4 macrocyclic complexes. Electrochimica Acta, 2014, 140, 314-319.	5.2	30
32	Optimizing the reactivity of surface confined cobalt N4-macrocyclics for the electrocatalytic oxidation of l-cysteine by tuning the Co(II)/(I) formal potential of the catalyst. Electrochimica Acta, 2014, 126, 37-41.	5.2	20
33	Determination of lactose by a novel third generation biosensor based on a cellobiose dehydrogenase and aryl diazonium modified single wall carbon nanotubes electrode. Sensors and Actuators B: Chemical, 2013, 177, 64-69.	7.8	46
34	Tuning the Fe(II)/(I) formal potential of the FeN4 catalysts adsorbed on graphite electrodes to the reversible potential of the reaction for maximum activity: Hydrazine oxidation. Electrochemistry Communications, 2013, 30, 34-37.	4.7	28
35	Osmium-Polymer Modified Carbon Nanotube Paste Electrode for Detection of Sucrose and Fructose. Materials Sciences and Applications, 2013, 04, 15-22.	0.4	4
36	Spectroscopic and Crystallographic Characterization of "Alternative Resting―and "Resting Oxidized― Enzyme Forms of Bilirubin Oxidase: Implications for Activity and Electrochemical Behavior of Multicopper Oxidases. Journal of the American Chemical Society, 2012, 134, 5548-5551.	13.7	50

Federico Tasca

#	Article	IF	CITATIONS
37	Effect of Deglycosylation of Cellobiose Dehydrogenases on the Enhancement of Direct Electron Transfer with Electrodes. Analytical Chemistry, 2012, 84, 10315-10323.	6.5	51
38	A third generation glucose biosensor based on cellobiose dehydrogenase from Corynascus thermophilus and single-walled carbon nanotubes. Analyst, The, 2011, 136, 2033-2036.	3.5	68
39	Cellobiose Dehydrogenase Aryl Diazonium Modified Single Walled Carbon Nanotubes: Enhanced Direct Electron Transfer through a Positively Charged Surface. Analytical Chemistry, 2011, 83, 3042-3049.	6.5	116
40	Wiring of pyranose dehydrogenase with osmium polymers of different redox potentials. Bioelectrochemistry, 2010, 80, 38-42.	4.6	60
41	Increasing the coulombic efficiency of glucose biofuel cell anodes by combination of redox enzymes. Biosensors and Bioelectronics, 2010, 25, 1710-1716.	10.1	84
42	Cellobiose Dehydrogenase: A Versatile Catalyst for Electrochemical Applications. ChemPhysChem, 2010, 11, 2674-2697.	2.1	175
43	Effect of Nanostructured Carbon Electrode Surfaces on the Percentage of Adsorbed Redox Enzyme Molecules in Direct Electron Transfer Contact. ECS Meeting Abstracts, 2010, , .	0.0	Ο
44	Comparison of Direct and Mediated Electron Transfer for Cellobiose Dehydrogenase from <i>Phanerochaete sordida</i> . Analytical Chemistry, 2009, 81, 2791-2798.	6.5	69
45	Tryptophan Repressor-Binding Proteins from Escherichia coli and Archaeoglobus fulgidus as New Catalysts for 1,4-Dihydronicotinamide Adenine Dinucleotide-Dependent Amperometric Biosensors and Biofuel Cells. Analytical Chemistry, 2009, 81, 4082-4088.	6.5	19
46	Increasing amperometric biosensor sensitivity by length fractionated single-walled carbon nanotubes. Biosensors and Bioelectronics, 2008, 24, 272-278.	10.1	35
47	Direct Electron Transfer at Cellobiose Dehydrogenase Modified Anodes for Biofuel Cells. Journal of Physical Chemistry C, 2008, 112, 9956-9961.	3.1	93
48	Highly Efficient and Versatile Anodes for Biofuel Cells Based on Cellobiose Dehydrogenase from <i>Myriococcum thermophilum</i> . Journal of Physical Chemistry C, 2008, 112, 13668-13673.	3.1	84
49	Amperometric Biosensors for Detection of Sugars Based on the Electrical Wiring of Different Pyranose Oxidases and Pyranose Dehydrogenases with Osmium Redox Polymer on Graphite Electrodes. Electroanalysis, 2007, 19, 294-302.	2.9	65
50	Direct electrochemistry and bioelectrocatalysis of H2O2 reduction of recombinant tobacco peroxidase on graphite. Effect of peroxidase single-point mutation on Ca2+-modulated catalytic activity. Journal of Electroanalytical Chemistry, 2006, 588, 112-121.	3.8	32